Thermochimica Acta, 174 (1991) 269–280
Elsevier Science Publishers B.V., Amsterdam

EPITAXIALLY GROWN CUPRATE SUPERCONDUCTOR FILMS AND FURTHER ATTEMPTS AT THEIR DESIGN

MAKI KAWAI

Research Laboratory of Engineering Materials, Tokyo Institute of Technology, 4259 Nagatsuta, Midori-ku, Yokohama 227 (Japan)

(Received 4 December 1989)

ABSTRACT

Epitaxially grown cuprate superconducting films are one of the most promising systems from the view-point of applications. The nature of the epitaxial growth of the film on the substrate surface, and heteroepitaxial thin film are discussed. Further artificial designing of the film by the layer-by-layer deposition method and a hint on designing a self-selective deposition system is discussed.

INTRODUCTION

Superconducting oxide crystals prepared in thin-film form are vital for fundamental physical studies as well as for device applications. From the very early stages of investigation of these materials, attempts at film formation of the cuprate superconductor have been approached using various methods.

Starting with LaSrCuO film formed by the sputtering method [1], physical processes such as molecular beam epitaxy (MBE) [2–4], laser ablation [5,6] and magnetron sputtering along with chemical processes such as chemical vapour deposition (CVD) [7,8], spray pyrolysis [9,10] and spin coating have been utilized. When we consider the cuprate superconductor film from a crystallographic viewpoint, it seems that much more perfect crystals have been obtained as thin films compared with the bulk single crystal. One of the advantages observed so far for the thin-film crystal is that the highest critical current (J_c) is obtained.

For applications, the critical current J_c needed for the power-on clip is said to be 5×10^6 A cm^{-2}. This value has been obtained in many YBaCuO films in zero field. A problem arises from the fact that J_c usually decreases when a field is applied. This is because grain boundaries in the crystal usually have a high resistivity and a heat problem arises from the areas, leading to a decrease in the critical current. High J_c values of the order of

0040-6031/91/$03.50

TABLE 1

Surface structure and lattice constants

Material	Index	Lattice constants (Å)
MgO	100	$a = b = 4.20$
$SrTiO_3$	100	$a = b = 3.91$
Si	100	$a = b = 3.84$
$Bi_2Sr_2CaCu_2O_x$		$a = b = 3.82$
$YBa_2Cu_3O_{7-x}$		$a = 3.83$
		$b = 3.89$

5×10^6 A cm^{-2} have been obtained, however, when the film is epitaxially grown to a high crystallographic quality. Growth of a highly epitaxial film usually depends on substrate selection. As a first principle, agreement of the lattice constants of the film to be grown with those of the substrate must be considered. The lattice constants of various cuprate superconductors and typical substrates used for film formation are listed in Table 1.

As is clearly seen from Table 1, $SrTiO_3$ has lattice constants quite similar to those of $YBa_2Cu_3O_{7-x}$ and BiSrCaCuO. MgO, which is the most frequently used substrate, has a large mismatch of 9%. The crystal growth of a cuprate superconductor on such substrates, especially in the very early stages, has a large influence on the quality of the film grown.

EPITAXIAL FILM GROWTH ON MgO

In spite of the large lattice mismatch, highly oriented epitaxial $YBa_2Cu_3O_{7-x}$ thin films were prepared on MgO(100) by molecular beam epitaxy at a substrate temperature of 550–600 °C. In situ growth was achieved by incorporating reactive oxygen species produced by a remote microwave plasma in a flow-tube reactor. The epitaxial (001) orientation was demonstrated by X-ray diffraction and ion channelling with a film thickness of 1000 Å [11]. Annealing in 1 atm of O_2 at 500 °C converted the oxygen content from 6.3 to 6.8. A question arises as to how the large lattice mismatch of 9% was relaxed during the epitaxial growth. In situ observation by reflection high-energy electron diffraction (RHEED) during the epitaxial growth of $YBa_2Cu_3O_{7-x}$ film on MgO(100) using reactive oxygen and molecular beam epitaxy seems to give an answer to this question. RHEED observation during the formation of the perovskite structure of $YBa_2Cu_3O_{7-x}$ from an initial deposit has been demonstrated [12]. A sharp streak in every deposition stage seems to indicate layer-by-layer growth. The initial deposit on the substrate of MgO (with a large mismatch of 9%) maintained the same in-plane lattice spacing as MgO. The lattice spacing

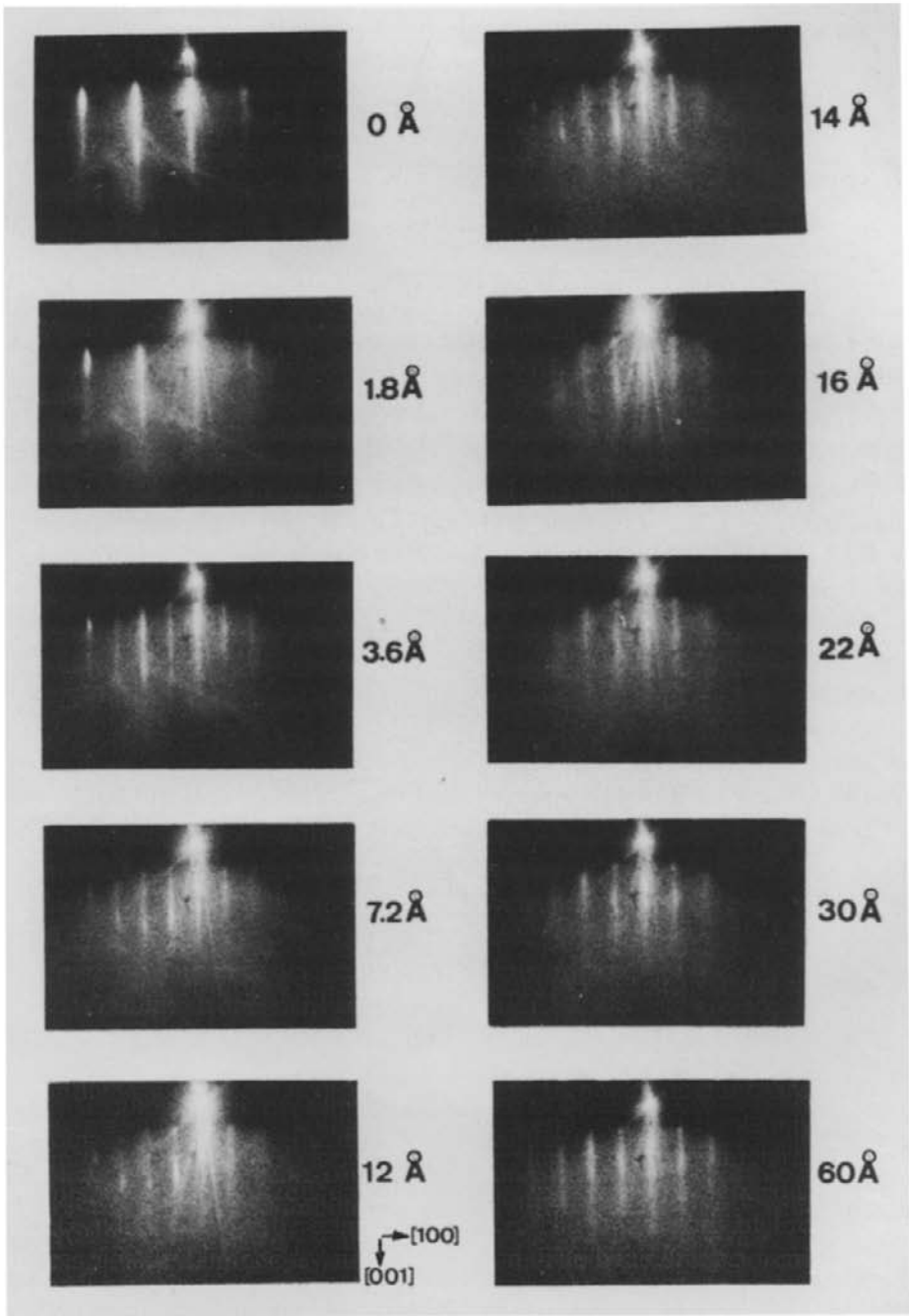

Fig. 1. In situ RHEED patterns observed during the growth of YBCO film on MgO(100). From ref. 12.

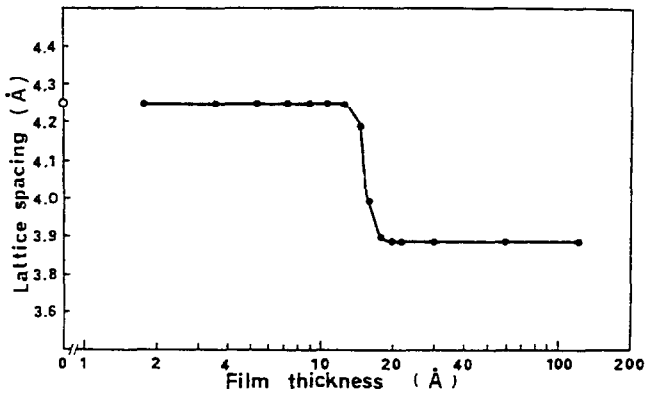

Fig. 2. Lattice spacing vs. thickness of YBCO film on MgO(100) calculated from the distances between the streaks. From ref. 12.

converted from the bulk value of MgO to that of $YBa_2Cu_3O_{7-x}$ when the layer became thicker than 12 Å, this value being similar to that of a c axis in $YBa_2Cu_3O_{7-x}$. Changes in the RHEED pattern and the lattice spacing of the film formed on MgO(100) are shown as a function of film thickness in Figs. 1 and 2 respectively.

ULTRATHIN FILMS

Even films having a thickness below 100 Å show superconductivity [12–14]. Observation of the superconducting properties in a limited number of Cu–O planes, containing only a few unit cells, enables us to determine

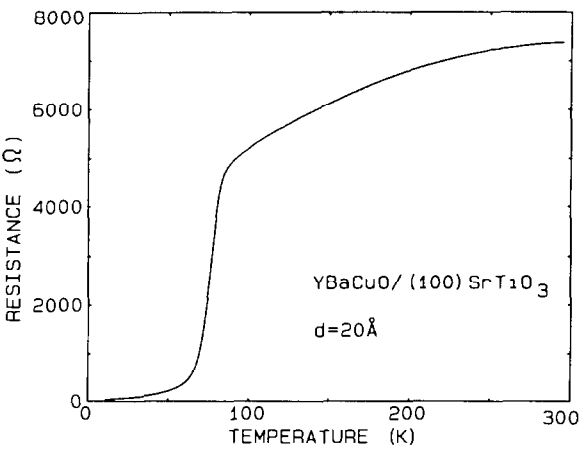

Fig. 3. Transition curve of an exceptionally good YBaCuO film 2 nm thick on (100)$SrTiO_3$. From ref. 15.

the properties of the Cu–O plane itself. Ultrathin films of $YBa_2Cu_3O_{7-x}$ having thicknesses down to 2 nm were grown on $SrTiO_3(100)$ and MgO(100) by inverted cylindrical magnetron sputtering [15]. Metallic behaviour and zero resistance temperatures above 4.2 K were obtained in films 3 nm thick on $SrTiO_3$ (Fig. 3). Thinner films revealed temperature-activated conductivity and only partial transitions to superconductivity owing to inhomogeneities in the film morphology. On MgO, the critical film thickness leading to deterioration of the transport properties was 6 nm. Ion scattering and backscattering measurements were performed on ultrathin films of $YBa_2Cu_3O_{7-x}$ on $SrTiO_3(100)$ and MgO(100). With a thickness of 90 Å, the

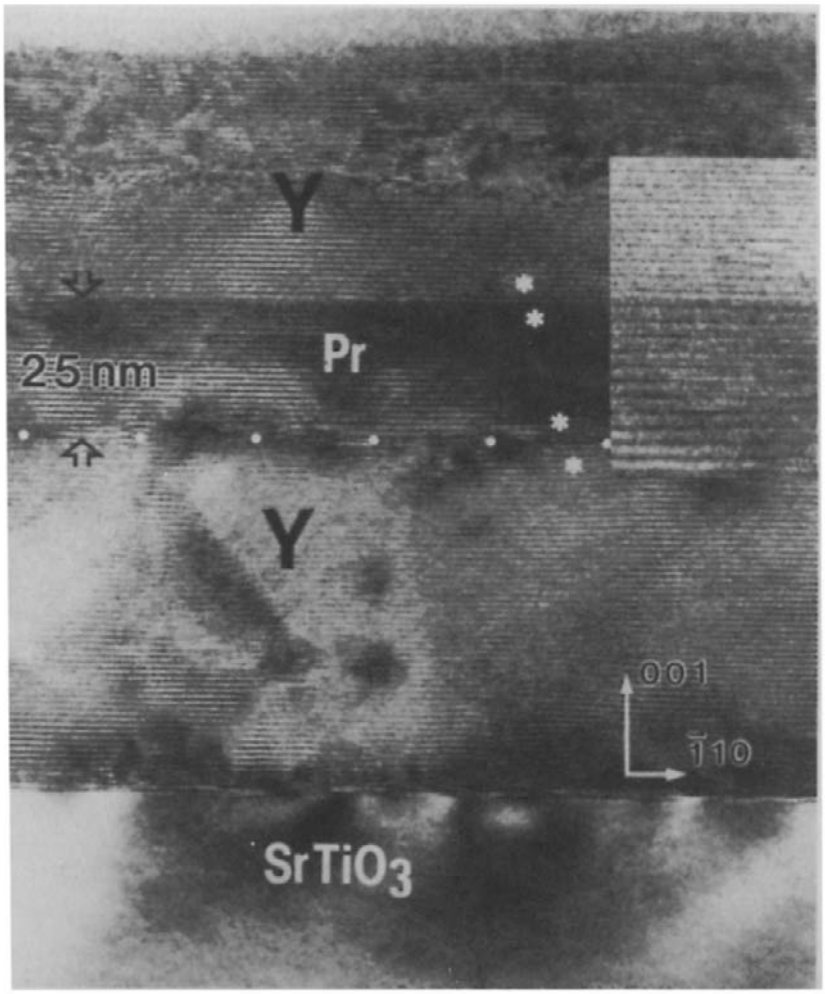

Fig. 4. Cross-sectional electron microscopy pictures of $YBa_2Cu_3O_7/25$ nm $PrBa_2Cu_3O_7/YBa_2Cu_3O_7$ on an $SrTiO_3(100)$ substrate. The interfaces are marked by arrows. From ref. 16.

minimum yield values χ_{min} were 43% and 65% on $SrTiO_3$ and MgO respectively. The difference in the χ_{min} values reflects the difference in the effect of dechannelling at the film–substrate interface. Using these ultrathin films, an analysis of fluctuation-enhanced conductivity near T_c in terms of the Aslamazov–Larkin theory revealed three-dimensional behaviour even in the thinnest fully superconducting films.

EPITAXIAL GROWN HETEROSTRUCTURAL FILMS

Epitaxial growth of the $YBa_2Cu_3O_7$ film has been established for various methods, including the system mentioned above. Thin films having high critical current densities have been obtained. As far as applications of the cuprate superconductors are concerned, films thus formed have to be made into devices. For this, a junction between the superconductor and the insulator or the semiconductor must be formed. Since the physical properties of these films are highly dependent on the quality of the crystal, these junctions have to be made in the sense of epitaxial growth of the hetero layers. Heteroepitaxial thin films of $YBa_2Cu_3O_7$ and $PrBa_2Cu_3O_7$ were produced by high oxygen pressure de-sputtering [16]. The superconducting properties of the $YBa_2Cu_3O_7$ layers were examined by resistivity and critical current measurements, and did not show any degradation due to the proximity of the $PrBa_2Cu_3O_7$ layers. The microstructure, interdiffusion and epitaxy of the heterostructures have been studied by cross-sectional transmission electron microscopy, Rutherford backscattering spectroscopy and helium-ion channelling. No interdiffusion at the interface between the different layers could be observed. The transmission electron microscopy of the epitaxially grown heterostructure of $YBa_2Cu_3O_7$ and $PrBa_2Cu_3O_7$ is shown in Fig. 4.

LAYER-BY-LAYER CONSTRUCTION OF ON OXIDE SUPERCONDUCTIVE FILM [17]

The superconducting properties of cupric oxide superconductors are known to depend strongly on the structural and electronic state of the CuO_2 sheet in the unit cell of the perovskite structure. Two types of carriers, electron and hole, are known for different materials and, in either case, the CuO_2 layer is considered to be the conductive layer. The framework of the perovskite structure is determined by its composition. The Madelung potential induced by the component ions, such as Ba, Sr, Y, Bi, Tl and Cu, together with the charge balance of the ions and anions including oxygen are said to be one of the causes for the carrier being in the CuO_2 sheet.

As the essential structure in the cuprate superconductor is the CuO_2 sheet, the atomic arrangement and the carrier density in the sheet are the most important functions to consider. The essential features of the CuO_2 sheet are the distance between the Cu and O atoms, the Cu–O–Cu angle and the appropriate number of charge carriers induced in the CuO_2 sheet. As a model for the two-dimensional CuO network in high T_c superconductor oxides, a DV-Xα calculation for the CuO_x ($x = 4$, 5 or 6) cluster was carried out [18]. By varying the hole density and the Cu–O bond lengths independently, Mulliken population analysis revealed that the electron was drawn out from the oxygen 2p at the plane site and not from the copper 3d nor from the oxygen at the apex site for each cluster. An increase in the electron density enhances the hybridization between the oxygen 2p and copper 3d orbitals, resulting in a rise in the overlap population between Cu and O atoms.

Accordingly, the properties of the copper-based superconductor can be modified by controlling the structure of the CuO_2 sheet and also the number

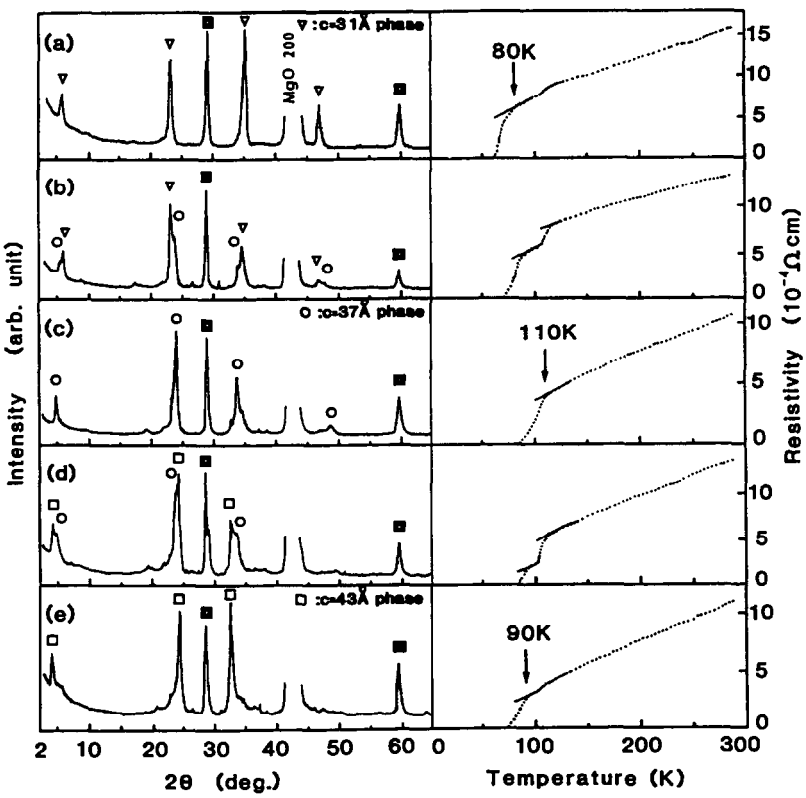

Fig. 5. X-ray diffraction patterns and temperature dependence of the resistivity after annealing of Bi–Sr–Ca–Cu–O thin films with various c-axis lattice spacings. From ref. 20.

of charge carriers. Such structural variation can be controlled by element substitution. In a bulk superconductor, whether the substitution takes place at a desired position or not merely depends on whether the structure desired is thermodynamically stable or not. Taking advantage of a sequential deposition technique, by shuttering in MBE or by switching the target in ion sputtering or laser ablation, a one-by-one construction of the oxide layer can be carried out [19].

Layer-by-layer construction of a cuprous oxide superconductor was first carried out in the Bi–Sr–Ca–Cu–O system [20,21]. Using multi-targets of alloys, Adachi et al. have shown that a CuO_2 sheet of 4 layers was constructed by this multi-target sputtering method [20]. By changing the sputtering time of a CaCu target, they succeeded in forming CuO_2 sheets of 2, 3 and 4 layers as desired. The T_c of the $n = 4$ phase was detected for the first time and the value was considered to be 90 K (Fig. 5). The idea of increasing the T_c value by increasing the number of sheets of CuO_2 thus

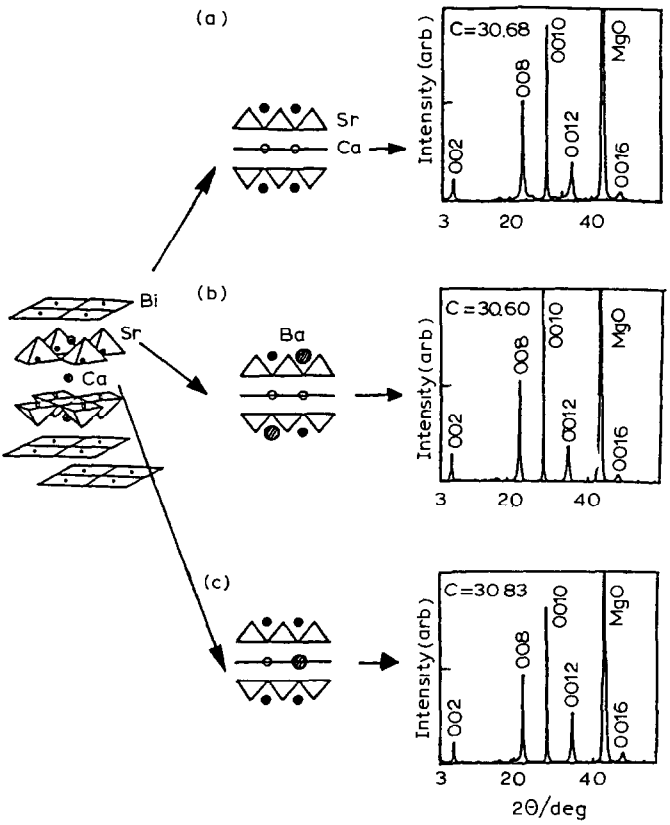

Fig. 6. Schematic representation of the partial substitution of Ba in Sr or Ca sites. a, BSCCO film without Ba substitution; b, partial substitution (30%) of Ba for Sr; c, substitution of Ba for Ca. From ref. 22.

disappeared. Other techniques such as laser ablation [21] and MBE [19] have been applied to layer-by-layer film formation. Whatever the technique, artificial control of the layer structure seems to succeed.

Apart from control of the number of CuO_2 layers, selective substitution of alkaline-earth elements has been applied [22]. The structural functions of interest are the distance between the CuO_2 layers, the Cu–O bond length in the plane and the distance between Cu and O(apex).

Carrier concentration can be controlled by the oxygen content and by the substitution by ions having a different valence state. The distance between the CuO_2 layers influences the interactions between the layers. Introducing larger alkaline-earth ions in place of Ca^{2+} may work. However, Ba^{2+} was not successfully introduced into the structure for the bulk material. Sequential deposition of elements by laser ablation was applied to film formation with Ba^{2+} substituted for Ca^{2+}. Figure 6 shows the X-ray diffraction pattern of the substituted film, showing that the larger the ion substituted for Ca^{2+}, the larger the cell constant for the *c* axis. Charge carrier concentration is also controlled by site-selective Pb doping in the Bi_2O_2 layer [22].

INTERACTION BETWEEN THE SUBSTRATES AND THE FIRST ATOMIC LAYERS: A SURFACE SCIENCE PROBLEM

Controlled layer deposition has been applied in forming a desired structure with partial success. It is of great interest to know how much artificial design of the layer structures is possible. There are many kinds of structural functions that we would like to vary. We shall consider such problems as choosing substrates, cleaning the surface, using the interaction of the substrate surface with deposited atoms to positively control the film structure (e.g. atomic distance), and the advantage of epitaxial growth.

Observation of the substrate surface at an atomic level and the behaviour of metals deposited onto the surface has become increasingly important. So far, substrates used for high-quality epitaxially grown films are limited to $SrTiO_3$ or MgO. One of the most interesting substrate materials for application is silicon. Even though the match in lattice constants is quite satisfactory, films grown on Si seem to have intermixing at the interface of the cuprate and Si. Since the surface of bare Si is covered with very reactive dangling bonds, an Si surface reacts with oxygen in the system to form amorphous SiO_2. Several systems are known to terminate the dangling bond of Si(111). As an example, passivating the dangling bonds with an atomic layer of Bi on the Si(100) surface has been demonstrated [23]. As shown in Fig. 7, an atomic layer of Bi deposited on a clean Si(100) surface completely reacts with the dangling bond, resulting in the formation of a passivated surface. Below the desorption temperature for the first Bi layer on Si, reaction with gaseous oxygen on this surface revealed that the Bi deposited

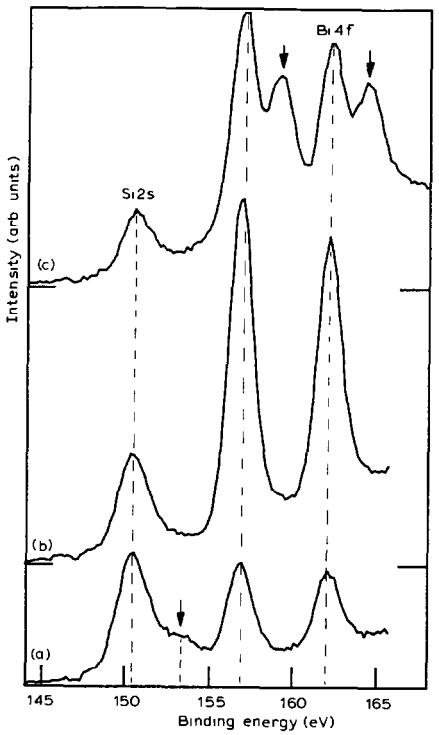

Fig. 7. X-ray photoelectron spectra of Bi/Si(001) after reaction with O_2 (10^{-4} Pa) at 500 °C. a, Bi < 1 ML (monolayer), showing only Si in an oxidized state; b, Bi = 1 ML, neither Si nor Bi is oxidized; c, Bi > 1 ML, only the excess Bi is oxidized. From ref. 23.

on the Si(100) surface could only be oxidized when the coverage exceeded one monolayer. Although cuprate layers have not been built on this surface, such a surface, completely passivated towards reaction with oxygen, must be considered for the epitaxial growth of cuprate on an Si surface.

FURTHER CONSIDERATIONS IN THE DESIGN OF REACTIONS FOR SELECTIVE DEPOSITION

In order to control the amount of surface deposition on an atomic scale, one of the most essential points is to stop the deposition just at the level needed for layer formation. In the case of MBE, most of the level of deposition is controlled by a shuttering technique. In this case, the sharpness of the cut-off of the source material usually determines the quality of the film. If the source material itself has some selectivity in its sticking properties, then the number of atoms can be controlled naturally. A good example of this is the formation of GaAs by the MBE method. The selective adsorption properties of these elements leads to formation of a sharp

interface between the Ga and As layers. In the case of high T_c oxide superconductors, these types of selective adsorption property have not been observed. It is extremely important to find some surface reaction where the elements are selectively deposited onto the desired surface. With this in mind, a reaction between a surface functional group and a metal-containing molecule was examined.

The model reaction examined was the reaction of $Cu(DPM)_2$ with OH on the surface of SiO_2 [24]. The $Cu(DPM)_2$ molecule selectively adsorbed onto the surface OH and reacted with the OH to give a surface chemisorbed state. The amount of adsorbed $Cu(DPM)_2$ was linear with the amount of surface OH. IR spectra of adsorbed species revealed that the surface OH and the dipivaloylmethanate (DPM) ring had reacted, and that the aromaticity of the ring had disappeared. The DPM ligand could be removed by reaction with H_2O at 400 °C, copper remained on the surface. It was shown that the $Cu(DPM)_2$ was selectively adsorbed onto the surface OH of the SiO_2 substrate, and by reacting with water molecules, a Cu atom was left on the surface.

CONCLUSIONS

Epitaxially grown cuprate superconducting films are vital for fundamental physical studies as well as for device applications. A heteroepitaxial system has been achieved and the future of these films seems promising. The artificial design of a cuprate system by layer-by-layer deposition has succeeded in forming new types of systems. Further attempts at atomic layer epitaxy with self-selective deposition methods are now in progress.

REFERENCES

1 M. Suzuki and T. Murakami, Jpn. J. Appl. Phys., 26 (1987) L524.
2 J. Kwo, T.C. Hsieh, R.M. Fleming, M. Hong, S.H. Lion, B.A. Davidson and L.C. Feldman, Phys. Rev. B, 36 (1987) 4039.
3 T. Terashima, K. Iijima, K. Yamamoto, Y. Bando and H. Mazaki, Jpn. J. Appl. Phys., 27 (1988) L91.
4 T. Terashima, Y. Bando, K. Iijima, K. Yamamoto and K. Hirata, Appl. Phys. Lett., 53 (1988) 2232.
5 D. Dijikkamp, T. Venkatesan, X.D. Wu, S.A. Shaheen, N. Jisrawi, H.Y. Lee, W.L. McLean and M. Croft, Appl. Phys. Lett., 51 (1987) 619.
6 M. Kanai, T. Kawai, M. Kawai and S. Kawai, Jpn. J. Appl. Phys., 26 (1988) L1746.
7 H. Yamane, H. Masumoto, T. Hirai, H. Iwasaki, K. Watanabe, N. Kobayashi, Y. Muto and H. Kurosawa, Appl. Phys. Lett., 53 (1988) 1548.
8 A.D. Barry, D.K. Gaskill, R.T. Holm, B.J. Cukanskas, R. Kaplan and R.L. Henry, Appl. Phys. Lett., 52 (1988) 1743.

9 M. Kawai, T. Kawai, H. Masuhira and M. Takahashi, Jpn. J. Appl. Phys., 26 (1987) L1746.
10 A. Gupta, G. Koren, E.A. Giess, N. Moore, E.J.M. O'Sullivan and E.I. Cooper, Appl. Phys. Lett., 52 (1987) 2077.
11 J. Kwo, M. Hong, D.J. Trevor, R.M. Fleming, A.E. White, R.-C. Farrow, A.R. Kortan and K.T. Short, Appl. Phys. Lett., 51 (1988) 2683.
12 T. Terashima, K. Iijima, K. Yamamoto, K. Hirata, Y. Bando and T. Takada, Jpn. J. Appl. Phys., 28 (1989) L987.
13 J. Schubert, U. Poppe and W. Sybertz, J. Less-Common Met., 151 (1989) 277.
14 T. Venkatesan, X.D. Wu, B. Dutta, A. Inam, M.S. Hedge, D.M. Hwang, C.C. Chang, L. Nazar and B. Wilkins, Appl. Phys. Lett., 54 (1989) 581.
15 X.X. Xi, J. Geerk, G. Linker, Q. Li and O. Meyer, Appl. Phys. Lett., 54 (1989) 2367.
16 C.J. Jia, B. Kabius, H. Soltner, U. Poppe, K. Urban , J. Schubert and Ch. Buchal, Physica C, 167 (1990) 463.
17 M. Kanai, T. Kawai and S. Kawai, Vacuum, (1989) submitted.
18 R. Sekine, M. Kawai and H. Adachi, Physica C, 159 (1989) 161.
19 D.G. Schlom, J.N. Eckstein, E.S. Hellman, S.K. Streiffer, J.S. Harris, Jr., M.R. Beasley, J.C. Bravman and T.H. Geballe, Appl. Phys. Lett., 53 (1988) 1660.
20 H. Adachi, S. Kohiki, K. Setsune, T. Mitsuya and K. Wasa, Jpn. J. Appl. Phys., 27 (1988) L1883.
21 M. Kanai, T. Kawai, S. Kawai and H. Tabata, Appl. Phys. Lett., 54 (1989) 1802.
22 H. Tabata, T. Kawai, M. Kanai, O. Murata and S. Kawai, Jpn. J. Appl. Phys., 28 (1989) L823.
23 T. Hanada and M. Kawai, Vacuum, 41 (1990) 650.
24 R. Sekine and M. Kawai, Appl. Phys. Lett., 56 (1990) 1466.